Paramagnetic Ions as Structural Probes in Solid-State NMR: Distance Measurements in Crystalline Lanthanide Acetates

Adrian R. Brough, Clare P. Grey,† and Christopher M. Dobson*

Contribution from the Inorganic Chemistry Laboratory, University of Oxford, South Parks Road, Oxford, OX1 3QR, UK

Received November 16, 1992

Abstract: The rare earth acetates $M(O_2CCH_3)_3{\cdot}4H_2O$ (M = Nd, Sm, Eu, Y) and $Pr(O_2CCH_3)_3{\cdot}H_2O$, and the analogous deuterated compounds, have been studied by ^{13}C MAS-NMR. The paramagnetic materials show a large range of isotropic ^{13}C chemical shifts which result largely from contact interactions with the rare earth electronic moments. They often show substantial linebroadening, which appears to result predominantly from anisotropic bulk magnetic susceptibility broadening for the deuterated compounds; the line widths for the protonated materials are increased further because of incomplete proton decoupling. Proton spectra acquired from a largely deuterated sample indicated that the spread in proton frequencies (40 kHz for $Sm(O_2CCH_3)_3{\cdot}4H_2O$ at 4.7 T, and calculated to be approximately 200 kHz for $Eu(O_2CCH_3)_3{\cdot}4H_2O$) is too large for decoupling to be effective with attainable ^1H power levels. The deuterated materials exhibit sufficiently good resolution to allow analysis of the large ^{13}C spinning sideband manifolds; these result mainly from dipolar coupling to the paramagnetic centers. X-ray diffraction shows that the solid solutions $Y_{(1-x)}Ln_x(O_2CCH_3)_3{\cdot}4H_2O$ (Ln = Pr, Nd, Sm, Eu; $x \leq 0.1$) crystallize with the $Y(O_2CCH_3)_3{\cdot}4H_2O$ crystal structure. MAS-NMR spectra of the ^{13}C enriched deuterated analogues contain remarkably narrow resonances of only 100 Hz line width despite having spinning sideband envelopes spanning 1000 ppm. The paramagnetic shift anisotropies could be predicted with reasonable accuracy by considering the interactions of the nuclei with the single nearest paramagnetic ion. Ln-^{13}C distances could also be estimated from the spectra and agreed to within 5% for the carboxyl carbons and 15% for the methyl carbons with the distances available from single-crystal X-ray diffraction studies. The different resonances in the solid solutions could then be assigned by the use of these estimated distances despite the large number of different ^{13}C local environments. These results suggest that in favorable circumstances, paramagnetic centers can provide a means for the determination of structural information and distances from MAS-NMR.

1. Introduction

NMR spectroscopy has become a standard technique for the determination of molecular structure in solution. High-resolution spectra of low molecular weight species can be obtained routinely from a wide range of nuclei, and multidimensional experiments enable the study of increasingly large and complex molecules.[1,2] A wide variety of approaches is then available to extract structural parameters from measurements of both scalar and dipolar couplings. Solid-state NMR spectroscopy[3] is, in contrast, a much less well developed method for structure determination although the geometric dependence of the magnitude of the dipolar coupling between nuclei has recently been exploited to obtain internuclear distances in an increasing number of experiments.[4-10] There have, however, been few attempts to utilize the much larger dipolar coupling that occurs between the electron and nuclear spins that can dominate the MAS spectra of paramagnetic materials, producing broad spinning sideband manifolds.

While paramagnetic ions have found widespread use in solution NMR spectroscopy as relaxation and shift probes,[11] many paramagnetic solids show poorly resolved spectra, and it has often been assumed that the introduction of paramagnetic ions into a solid system will result in a severe loss of resolution, for example because of short nuclear relaxation times. The ^{13}C relaxation properties of members of the lanthanide acetate series have, however, been measured;[12] the short relaxation times were shown to account for only a small part of the large line widths. We have recently postulated that a major contribution to the linebroadening observed in these spectra is not intrinsic but results from an inability to decouple the protons completely,[13] since the removal of protons by deuteration[14] leads to greatly reduced line widths in the ^{13}C MAS-NMR spectra. This suggests that under appropriate conditions high-resolution spectra of many paramagnetic species may be recorded and analyzed.

MAS spectra have now been obtained from an increasing range of paramagnetic materials.[15-23] There have been few attempts to extract the spatial information contained in the spinning sideband manifolds; many of the previous studies of the overall shift anisotropy (SA) in paramagnetic solids have been performed on single crystals, or by analysis of powder lineshapes. For

* Author to whom correspondence should be addressed.
† Present address: DuPont Central Research and Development, Experimental Station Building 356, Wilmington, DE 19880-356.

(1) Derome, A. E. "*Modern NMR Techniques for Chemistry Research*; Pergamon Press: Oxford, UK, 1987.
(2) Wüthrich, K. *Acc. Chem. Res.* **1989**, *22*, 36.
(3) Fyfe, C. A. *Solid State NMR for Chemists*; C. F. C. Press: Guelph, 1983.
(4) Munowitz, M. G.; Griffin, R. G. *J. Chem. Phys.* **1982**, *76*, 2848.
(5) Yannoni, C. S.; Kendrick, R. D. *J. Chem. Phys.* **1981**, *74*, 747.
(6) Raleigh, D. P.; Levitt, M. H.; Griffin, R. G. *Chem. Phys. Lett.* **1988**, *146*, 71.
(7) Tycko, R.; Dabbagh, G. *Chem. Phys. Lett.* **1990**, *173*, 461.
(8) Gullion, T.; Schaefer, J. *J. Magn. Reson.* **1989**, *81*, 196.
(9) Herzog, B.; Hahn, E. L. *Phys. Rev.* **1956**, *103*, 148.
(10) Kaplan, D. E.; Hahn, E. L. *J. Phys. Radium* **1958**, *19*, 821.
(11) Williams, R. J. P. *Structure and Bonding* **1982**, *50*, 79.
(12) Ganapanthy, S.; Chacko, V. P.; Bryant, R. G.; Etter, M. C. *J. Am. Chem. Soc.* **1986**, *108*, 3159.
(13) Clayton, A. N.; Dobson, C. M.; Grey, C. P. *J. Chem. Soc., Chem. Commun.* **1990**, 72.
(14) Eckman, R. *J. Chem. Phys.* **1982**, *76*, 2767.
(15) Rundle, R. E. *J. Am. Chem. Soc.* **1957**, *79*, 3372.
(16) Jarrett, P. S.; Sadler, P. J. *Inorg. Chem.* **1991**, *30*, 2098.
(17) Oldfield, E.; Kinsey, R. A.; Smith, K. A.; Nichols, J. A.; Kirkpatrick, R. J. *J. Magn. Reson.* **1983**, *51*, 325.
(18) Campbell, G. C.; Haw, J. F. *Inorg. Chem.* **1988**, *27*, 3706.
(19) Walter, T. H.; Oldfield, E. *J. Chem. Soc., Chem. Commun.* **1987**, 646.
(20) Campbell, G. C.; Reibenspies, J. H.; Haw, J. F. *Inorg. Chem.* **1991**, *30*, 171.
(21) Haw, J. F.; Campbell, G. C. *J. Magn. Reson.* **1986**, *66*, 558.
(22) Groombridge, C. J.; Perkins, M. J. *J. Chem. Soc., Chem. Commun.* **1991**, 1164.
(23) Campbell, G. C.; Crosby, R. C.; Haw, J. F. *J. Magn. Reson.* **1986**, *69*, 191.

0002-7863/93/1515-7318$04.00/0

example, in an early study,[24] Bloembergen analyzed the orientation dependent ^1H shifts in a single crystal of $CuSO_4 \cdot 5H_2O$ at low temperatures. Single crystals are not, however, available for many compounds, and analysis of powder spectra is often difficult because of the need to deconvolute powder patterns from different resonances. McGarvey and Nagy[25,26] have investigated the temperature dependence of static powder ^1H spectra of $U(C_8H_8)_2$, a system where all the protons are chemically equivalent.

MAS allows separation of resonances in spectra with overlapping powder patterns; the overall shift anisotropy information is then contained in the sidebands. Nayeem and Yesinowski[27] have made use of this information in an investigation of polycrystalline $CuCl_2 \cdot 2H_2O$; they were able to estimate the degree to which paramagnetic electron density is delocalized from the copper ion onto the chloride ions by analysis of ^1H MAS spectra acquired from residual protons in a largely deuterated sample.

Anisotropic interactions other than the dipolar coupling between the electronic moment and the nucleus may be present. For example, we have previously obtained both ^{89}Y and ^{119}Sn MAS–NMR spectra from the lanthanide stannates $Ln_2Sn_2O_7$,[28-30] where both the high bulk magnetic susceptibilities of these materials and possible contributions from the anisotropic part of the contact shift contribute to the shape of the spinning sideband envelopes. In the present work, and in our study[31] of the compound $NaLn(edta) \cdot 8H_2O$, we have chosen to examine ionic molecular crystals where such effects should be much reduced, as a consequence of the much smaller hyperfine shifts observed in the ^{13}C MAS–NMR spectra of these materials, and their relatively low bulk magnetic susceptibilities.

In this paper, we investigate the causes of the large line widths found in MAS spectra of paramagnetic materials and devise methods for obtaining well resolved spectra. ^1H MAS–NMR spectra of the lanthanide acetates were obtained in order to determine directly whether the ^1H tensors are sufficiently large to prevent effective ^1H decoupling in the ^{13}C CPMAS–NMR spectra of these materials. The ^{13}C MAS–NMR spectra of the deuterated lanthanide acetates studied in this work are sufficiently well resolved that sideband analysis to determine the extent of the large shift anisotropies can be attempted. We show that for some resonances dipolar coupling is sufficiently large in relation to other interactions that it becomes the dominant factor determining the overall shift anisotropies. Solid solutions containing low concentrations of paramagnetic ions in a diamagnetic host are shown to give spectra with line widths that are almost as narrow as those observed in some equivalent diamagnetic materials.

2. Materials and Methods

All chemicals used were obtained from the Aldrich Chemical Co. The acetates $M(O_2CCH_3)_3 \cdot nH_2O$ (M = Pr, Nd, Sm, Eu, Y) were prepared by boiling a slight excess of the appropriate metal oxide (99.99%) with a mixture of 50% acetic acid and 50% deionized water. Excess oxide was removed by filtration, and the solutions were left to crystallize. The compounds were then recrystallized from 2% acetic acid. The solid solutions were prepared using the appropriate mixture of metal oxides. For the deuterated compounds, 99.9% deuterium oxide and 99.95% deuterated acetic acid (CD_3CO_2D) were used. The partially deuterated compound (where 3% of the deuterated methyl groups were replaced by protonated methyl groups) was prepared in the same manner, using a mixture of 3% of CH_3CO_2H and 97% of 99.95% CD_3CO_2D; 99.9% deuterium oxide was used as the solvent, both for preparation and for recrystallization. ^{13}C enriched samples were prepared from acetic acid enriched in ^{13}C to approximately 10% either at the methyl or at the carboxyl group. The acetic acids were prepared from the 100% ^{13}C enriched sodium salts by distilling a mixture of the salt, water (or deuterium oxide), and phosphoric acid and collecting the fraction boiling below 85 °C. The 100% ^{13}C enriched acetic acids were diluted with unenriched acetic acid to achieve the desired degree of enrichment.

All compounds were characterized by X-ray powder diffraction, using a Philips PW 1710 diffractometer. The X-ray powder patterns were compared with those recorded in the literature and also with those generated using the computer program LAZY PULVERIX[32] with atomic coordinates obtained from single-crystal studies of lanthanide acetates.[33-35] The homogeneity of the solid solutions was checked by X-ray emission analysis using a JEOL 2000FX analytical electron microscope. The solid solutions made were found to be homogeneous, with all crystallites having the same composition within experimental error.

Evaporation at room temperature of solutions of the stoichiometric yttrium, samarium, and europium acetates gave tetrahydrate crystals. A mixture of hydrates was formed for neodymium acetate, and the monohydrate was formed for praseodymium acetate. All the solid solutions $Y_{(1-x)}Ln_x(O_2CCD_3)_3 \cdot 4D_2O$ (Ln = Sm, Eu, Pr, Nd) were found to crystallize with the tetrahydrate structure even when 10% of the yttrium ions were substituted with Pr^{3+}, Eu^{3+}, or Nd^{3+}.

The NMR spectra were obtained using a Bruker MSL200 spectrometer (field 4.7 T; operating frequencies, ^1H, 200 MHz; ^{13}C; 50.3 MHz) and a Bruker MSL400 spectrometer (field 9.4 T; operating frequencies, ^1H; 400 MHz, ^{13}C, 100.6 MHz). Unless otherwise stated, all line widths and anisotropies refer to spectra acquired at 4.7 T. All chemical shifts were referenced externally to tetramethylsilane (TMS). Spectra were obtained from powdered materials packed in zirconia rotors, using MAS speeds of between 2 and 5.5 kHz. CPMAS with short contact times of typically 0.5 ms and rf field strengths of typically 60 kHz (for ^1H and ^{13}C) was used to obtain spectra from the protonated samples. Single pulse acquisition with small (20–40°) flip angles was used for the deuterated samples.

The spectral baselines were manually corrected where necessary. The very large spectral widths (up to 125 kHz at 4.7 T) employed to collect these spectra required fast digitization, resulting in distortion of the first few points of the FID from probe ringdown and receiver deadtime. Attempts to make use of rotationally synchronized Hahn echoes to overcome these problems were without success. The problems of overlap and of background signals were overcome by selective ^{13}C enrichment of either the methyl group or of the carboxyl group. The carboxyl or methyl resonances could then be detected separately, and the improved signal-to-noise ratio allowed an increased range of local environments, such as those found in the solid solutions, to be studied.

Spectral simulations were performed using Fortran-77 code on a VAX cluster at the Oxford University Computing Service. The programs make use of NAG[36] algorithms to diagonalize matrices, to determine eigenvectors, to generate random numbers, and to perform Fourier transforms. The program FSPIN[37] was

(24) Bloembergen, N. *Physica* **1950**, *16*, 95.
(25) McGarvey, B. R.; Nagy, S. *Inorg. Chem. Acta.* **1987**, *139*, 319.
(26) McGarvey, B. R.; Nagy, S. *Inorg. Chem.* **1987**, *26*, 4198.
(27) Nayeem, A.; Yesinowski, J. P. *J. Chem. Phys.* **1988**, *89*, 4600.
(28) Grey, C. P.; Smith, M. E.; Cheetham, A. K.; Dobson, C. M.; Dupree, R. *J. Am. Chem. Soc.* **1990**, *112*, 4670.
(29) Grey, C. P.; Dobson, C. M.; Cheetham, A. K.; Jakeman, R. J. B. *J. Am. Chem. Soc.* **1989**, *111*, 505.
(30) Cheetham, A. K.; Dobson, C. M.; Grey, C. P.; Jakeman, R. J. B. *Nature* **1987**, *328*, 706.
(31) Brough, A. R.; Grey, C. P.; Dobson, C. M. *J. Chem. Soc., Chem. Commun.* **1992**, 742.
(32) Yvon, K.; Jeitschko, W.; Parté, E. *LAZY PULVERIX*; Geneva, 1977.
(33) Favas, M. C.; Kepert, D. L.; Skelton, B. W.; White, A. H. *J. Chem. Soc., Dalton Trans.* **1980**, 454.
(34) *Gemelin Handbook of Inorganic Chemistry*, Birnbaum, E. R., Ed.; 8th ed.; 1980; Vol. D5.
(35) Ribot, F.; Toledano, P.; Sanchez, C. *Inorg. Chim. Acta* **1991**, *185*, 239.
(36) Numerical Algorithms Group (NAG) *Fortran Library, Mk 14*; 1988.
(37) Clayden, N. J.; Twyman, J. M. *FSPIN*; University of Oxford, 1989.

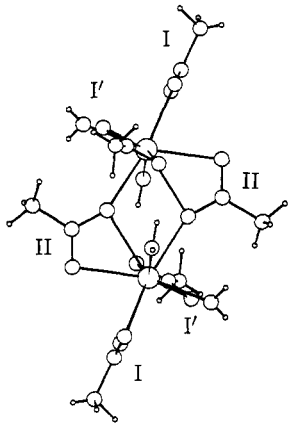

Figure 1. The structure of crystalline $Y(O_2CCH_3)_3{\cdot}4H_2O$ determined by a single crystal X-ray diffraction study.[35] It consists of $Y_2(O_2CCH_3)_6{\cdot}4H_2O$ dimers with the additional water molecules incorporated into the lattice. The dimers have a center of inversion between the metal ions, and there is one dimeric unit in the unit cell, so that in the stoichiometric compound there are three crystallographically distinct acetate groups. Chelated to each metal ion there are four acetate groups and two water molecules; three of the acetate groups are bidentate, while one acetate group, and both water molecules, are monodentate, giving 9-fold coordination overall. Two of the three bidentate acetate groups only chelate this one metal ion, and we designate them type I ligands; they are not symmetry related, and the two ligands (I and I') have slightly different environments. The remaining bidentate acetate group also coordinates the adjacent metal ion in the dimer in a monodentate manner, and we designate it a type II (bridging) ligand. In the event of the symmetry being reduced, as for example in the solid solutions which contain $YLn(O_2CCH_3)_6{\cdot}4H_2O$ dimeric units, then all six acetate groups will become crystallographically distinct. We then designate the ligands by the type I, I', or II label and a subscript indicating the identity of the metal ion chelated in a bidentate manner; e.g., type II_{Eu} for an acetate ligand chelated to an europium ion and bridging to an yttrium ion in a $YEu(O_2CCH_3)_6{\cdot}4H_2O$ dimer. The diagram was produced from the coordinates for $Gd(O_2CCH_3)_3{\cdot}4H_2O$[33] taken from the Cambridge Crystallographic Database.[41] X-ray powder diffraction shows the structures of $M(O_2CCH_3)_3{\cdot}4H_2O$, (M = Y, Sm, Eu, Gd, Lu) to be isomorphous.

used to determine the shift tensors from experimental data. It uses the theory of Maricq and Waugh[38] to calculate one rotational echo for a particular SA tensor. Powder averaging is performed over the three Euler angles, and a series of the echoes concatenated to form an FID, which is multiplied by a suitable window function. After Fourier transformation, the intensities of the spinning sidebands are least-squares fitted to the experimental data using the AMOEBA algorithm[39] and repeating the simulation to find the SA tensor that gives the best fit. FSPIN does not allow for the effects of imperfect spectral excitation, resulting from finite pulse lengths, nor for magnetic susceptibility broadening of spectra. The program ARBPARAMAG[40] was used to calculate the dipolar coupling between the nucleus of interest and all paramagnetic nuclei within a given radii. It requires the magnetic susceptibility tensor, unit cell dimensions, and fractional atomic coordinates of the paramagnetic species and is described more fully later in this paper.

3. Results

3.1. ^{13}C MAS–NMR Spectra of Stoichiometric Compounds. The structure[35,41] of crystalline $Y(O_2CCH_3)_3{\cdot}4H_2O$ is shown in Figure 1, and the figure caption indicates the notation used in this paper to describe the structure. A ^{13}C CPMAS–NMR spectrum of yttrium acetate tetrahydrate, $Y(O_2CCH_3)_3{\cdot}4H_2O$, is shown in Figure 2a. The line widths in this diamagnetic compound are less than 100 Hz, and resonances from all three crystallographically distinct acetate groups in the asymmetric unit are resolved. Samples of yttrium acetate prepared using different sources of yttrium oxide were found to exhibit variable line widths; the resolution achieved in the spectrum shown in Figure 2a is only observed if the compound is free of the

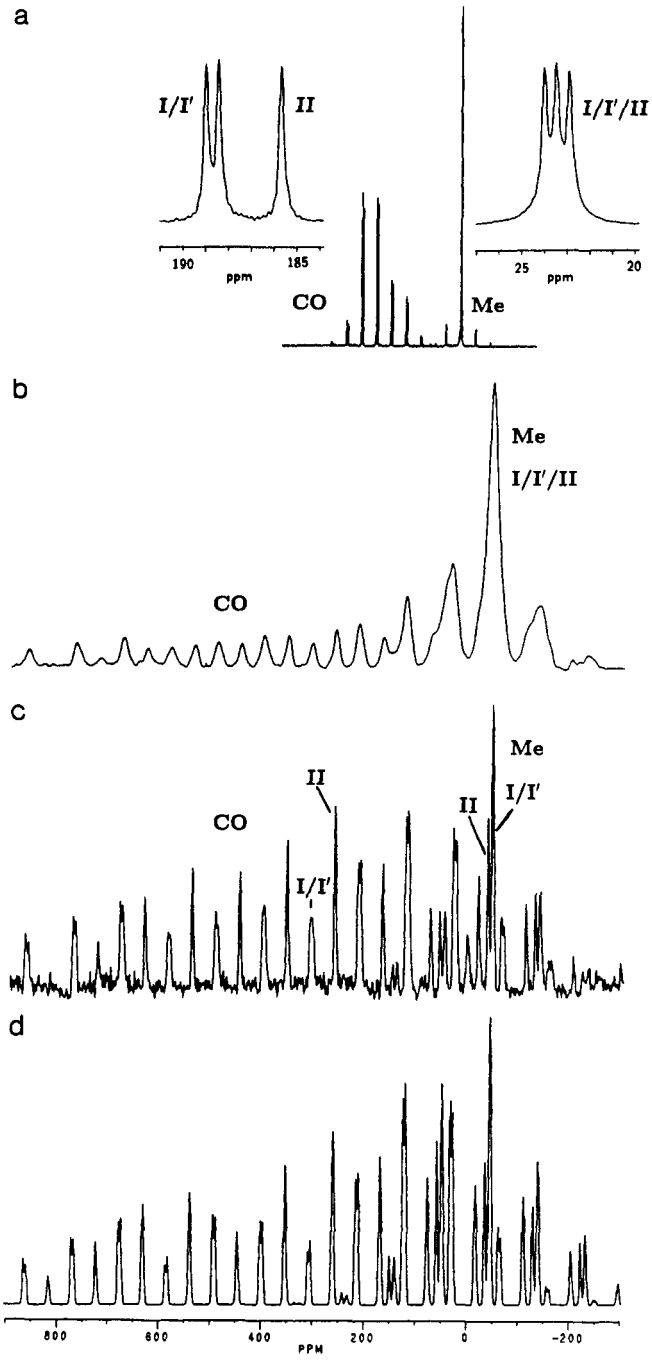

Figure 2. ^{13}C MAS–NMR spectra of (a) $Y(O_2CCH_3)_3{\cdot}4H_2O$ (CPMAS), (b) $Eu(O_2CCH_3)_3{\cdot}4H_2O$ (CPMAS), and (c) $Eu(O_2CCD_3)_3{\cdot}4D_2O$ (MAS) recorded at rotation rates of 1464, 4650, and 4650 Hz, respectively. The spectra are processed with (a) 5 and (b) 100 Hz of exponential linebroadening, and (c) is processed with 60 Hz of resolution enhancement. The isotropic peaks are labeled with their chemical shifts; remaining peaks are spinning sidebands. Spectrum (d) is calculated using the tensors given in Table II and applying an appropriate convolution to the FID for each resonance to simulate the isotropic shift and line width observed in the experimental spectrum.

(38) Maricq, M. M.; Waugh, J. S. *J. Chem. Phys.* **1979**, *70*, 3300.
(39) Press, W. H.; Flannery, B. P.; Teukolsky, S. A.; Vetterling, W. T. *Numerical Recipies*; Cambridge University Press: UK, 1986.
(40) Brough, A. R.; Grey, C. P.; Dobson, C. M. *ARBPARAMAG*; University of Oxford, 1989.
(41) Crystallographic Data Centre *Cambridge Crystallographic Database*; University Chemistry Laboratory, Cambridge, June 1992.

paramagnetic impurities found in lower grades (<99.99% purity) of commercial samples of yttrium oxide.

The three carboxyl resonances observed in the narrow range of shifts from 185–189 ppm can be divided into two types. Two of the resonances have similar shifts, in the range 188–189 ppm, and are likely to arise from the type I groups; the type II (bridging) groups probably produce the resonance with a distinct chemical shift of approximately 185 ppm. The three methyl resonances all fall in the range from 22–24 ppm and are only just resolved; it is not possible to assign them on the basis of chemical shift information alone.

The ^{13}C CPMAS spectrum of the homologous lanthanide compound, $Eu(O_2CCH_3)_3{\cdot}4H_2O$ is shown in Figure 2b. The line widths have significantly increased relative to the spectrum of the diamagnetic compound (to approximately 1200 Hz for the methyl groups and 900 Hz for the carboxyl groups). The dispersion of isotropic shift has also increased, however, so that the isotropic carboxyl groups resonate between 260 and 310 ppm and the methyl groups between –45 and –35 ppm. Large spinning sideband manifolds are observed; these lead to overlap between the spinning sideband envelopes associated with the methyl and carboxyl resonances. The signal-to-noise ratio is reduced as a consequence both of the large line width of each sideband and the large number of spinning sidebands. The short relaxation times of the ^{13}C nuclei, however, enabled the use of short recycle delays, making it possible to acquire more transients in a given time than for the homologous diamagnetic compound. We have also obtained ^{13}C MAS spectra of $Eu(O_2CCH_3)_3{\cdot}4H_2O$ with rotationally synchronized variation of phase (RSVP) ^1H decoupling[42,43] and with decoupling at two frequencies.[44] In both cases we observe somewhat narrower line widths than in spectra obtained without decoupling.

The ^{13}C MAS spectrum of the deuterated compound $Eu(O_2CCD_3)_3{\cdot}4D_2O$ is shown in Figure 2c. Line widths of approximately 200 Hz for the carboxyl resonances and of 400 Hz for the methyl resonances are observed (see Table I). In contrast to the spectrum of $Eu(O_2CCH_3)_3{\cdot}4H_2O$ (Figure 2b), there is little overlap between spinning sidebands associated with different isotropic resonances. There are two groups of isotropic resonances, one in the region 300–310 ppm which has very broad associated spinning sideband manifolds and the other centered around –40 ppm, with somewhat narrower sideband envelopes. Since resonances from atoms closer to the paramagnetic species are expected to show larger shifts and shift anisotropies, we assign the group of resonances at about 300 ppm to the carboxyl groups and the group at about –40 ppm to the methyl groups. This is in agreement with previous assignments for the trihydrate based on ^{13}C T_1 measurements.[12] As in the case of the diamagnetic compound it is possible to distinguish between resonances from type I and type II (bridging) acetate groups. Peaks in the ^{13}C MAS–NMR spectrum of $Eu(O_2CCD_3)_3{\cdot}4D_2O$ at –45 and –35 ppm have intensities in the ratio of approximately 2:1. This is consistent with their assignments as type I methyl groups and type II (bridging) methyl groups, respectively. Similarly, for the carboxyl groups, there are two closely spaced isotropic peaks in the region 300–310 ppm, with similar spinning sideband envelopes, which may be assigned to type I carboxyl groups, and one resonance at 260 ppm with a distinct spinning sideband envelope, which may be assigned to the type II (bridging) carboxyl groups.

Since the ^{13}C T_1's are short and the line widths are relatively narrow, signal-to-noise ratios were reasonable for the deuterated acetates, even though CP was no longer possible; the ^{13}C MAS spectra of the deuterated stoichiometric compounds and the CPMAS spectra of the equivalent protonated compounds presented in this paper both had acquisition times of approximately 8 h.

(42) Pratum, T. K. *J. Magn. Reson.* **1990**, *88*, 384.
(43) Pratum, T. K. *Chem. Phys. Lett.* **1990**, *172*, 291.

Table I. Experimental ^{13}C Line Widths Obtained in MAS–NMR Spectra of the Stoichiometric Compounds $Ln(O_2CCH_3)_3{\cdot}4H_2O$ and the Solid Solutions $Y_{(1-x)}Ln_x(O_2CCD_3)_3{\cdot}4D_2O$ (Ln = Nd, Pr, Eu) for Protonated (H) and Deuterated (D) Samples[a]

	^{13}C linewidths (Hz)		
compound	carboxyl	methyl	relative anisotropy[d]
Y(H)	61, 31	86	
Sm(H)	122, 107	153	
Sm(D)	76, 71	107	0.7
Nd(H)	*c*	1480	
Nd(D)	503, 229	427	4.2
$Nd_{0.1}Y_{0.9}$(D)	*c*	122, 107	
Eu(H)	970, 730	1190	
Eu(D)	260, 214	230, 366	4.0
$Eu_{0.1}Y_{0.9}$(D)	76–97	137, 104	
Pr(H)[b]	(840, 870)	(1150, 1350)	
Pr(D)[b]	(592, 610)	(806, 834)	11.0
$Pr_{0.05}Y_{0.95}$(D)	91–99	122–137	

[a] For solid solutions, the line widths given are for the paramagnetically shifted resonances only. [b] Stoichiometric $Pr(O_2CCH_3)_3{\cdot}nH_2O$ forms the monohydrate, and so the line widths for this compound are not directly comparable with those for the other compounds. [c] These compounds were not studied in detail; line widths for the methyl groups were measured from samples enriched in ^{13}C at the methyl groups. [d] Relative values for the anisotropy of the magnetic susceptibility (from Bleaney[45]).

The spinning sideband manifolds of the resonances in the spectra described above have been analyzed, to enable estimates of the shift anisotropies to be obtained. Analysis of the methyl group resonances was complicated by overlap with spinning sidebands from the carboxyl group resonances. This was overcome by selective ^{13}C enrichment of the methyl groups, which also confirmed the relative assignments of the methyl and carboxyl resonances. Tables I and II give a summary of the results obtained by analysis of the spectra acquired from the natural abundance and ^{13}C enriched stoichiometric compounds of Eu^{3+} described above and for compounds of the other lanthanide ions studied.

3.2. ^{13}C MAS–NMR Spectra of Solid Solutions. Spectra of solid solutions containing a small fraction of lanthanide ions in a diamagnetic host of yttrium acetate $Ln_xY_{(1-x)}(O_2CCD_3)_3{\cdot}4D_2O$ (Ln = Pr, Nd, Eu, Sm; $0 < x \leq 0.1$) have been recorded. Figure 3 shows the ^{13}C MAS spectrum obtained from $Eu_{0.1}Y_{0.9}(O_2CCD_3)_3{\cdot}4D_2O$ using 10% ^{13}C enrichment of the carboxyl groups and deuteration to maximize the sensitivity and resolution. Figure 4 shows the ^{13}C MAS spectrum of a deuterated sample enriched in ^{13}C at the methyl group.

In these spectra we can distinguish two major classes of resonance. Firstly, resonances are observed at the same isotropic shifts as those of the diamagnetic compound. Secondly, resonances having large paramagnetically induced shifts are observed. The resonances having the same shifts as the diamagnetic compounds have a T_1 of approximately 10 s but are broadened to about 150 Hz; additionally there appears to be a range of peaks showing small paramagnetic shifts. Hence the individual components of the resonance at ca. 188 ppm are not resolved. Analysis of the shift anisotropies of these resonances was not possible, since the peaks consisted of a number of overlapping resonances, preventing measurement of the sideband intensities for individual resonances.

All the shifted resonances in $Eu_{0.1}Y_{0.9}(O_2CCD_3)_3{\cdot}4D_2O$ have isotropic peak line widths of approximately 100 Hz, which is only about 30 Hz wider than in the corresponding diamagnetic compound. There are five well resolved shifted resonances in the MAS spectrum of $Eu_{0.1}Y_{0.9}(O_2CCD_3)_3{\cdot}4D_2O$ selectively enriched in ^{13}C at the *carboxyl* groups; for the *methyl* enriched compound, there are two resolved shifted resonances. Line widths and isotropic shifts of the shifted resonances for all the solid solutions studied are given in Tables I and III, respectively. For samples of $Y_{(1-x)}Sm_x(O_2CCD_3)_3{\cdot}4D_2O$, paramagnetically shifted reso-

Table II. Calculated and Experimental Shift Anisotropy (SA) Tensors for the Methyl (Me) and Carboxyl (CO) Groups in the Compounds $Ln(O_2CCD_3)_3{\cdot}4D_2O$ (Ln = Eu, Sm)[a]

	experimental SA		paramagnetic SA		overall SA	
compound	$\Delta_{(ppm)}$	η	$\Delta_{(ppm)}$	η	$\Delta_{(ppm)}$	η
			$Eu(O_2CCD_3)_3{\cdot}4D_2O$			
I/I'(CO)	695	0.37	739	0.34	660	0.64
	695	0.37	738	0.17	654	0.18
II(CO)	−532[d]	0.89	541	0.97	543	0.92
I/I'(Me)	180	0.65	227	0.46	238	0.33
	180	0.65	216	0.85	222	0.79
II(Me)	200	0.90	250	0.89	241	0.87
I/I'(H)	*b*		198	0.59	*c*	
			190	0.83		
II(H)			224	0.51		
			$Sm(O_2CCD_3)_3{\cdot}4D_2O$			
I/I'(CO)	−175	0.65	141.8	0.34	63.0	0.25
	−175	0.65	137.7	0.17	54.1	0.40
II(CO)	190	0.6	106.7	0.97	124.2	0.81
I/I'(Me)	43	0.85	45.4	0.46	56.0	0.28
	43	0.85	39.7	0.85	48.2	0.83
II(Me)	51	0.94	54.6	0.89	48.4	0.60
I/I'(H)	*b*		40	0.59	*c*	
			38	0.83		
II(H)			45	0.51		

[a] We use the notation $\Delta = \sigma_{11} - \sigma_{iso}$ and $\eta = (\sigma_{22} - \sigma_{33})/\Delta$. Paramagnetic SA: shift anisotropy calculated allowing for coupling to the maramagnetic moments only. Overall SA: SA calculated allowing both for the paramagnetic SA, and for the CSA tensor (determined from $Y(O_2CCH_3)_3{\cdot}4H_2O$) aligned conventionally (see text). Experimental SA: estimate of the overall SA obtained by analysis of the spinning sideband envelope of the observed spectra using the program FSPIN.[37] [b] Analysis of these spectra was not possible due to the large contribution from homonuclear dipolar coupling. [c] These data were not calculated. [d] The calculated and experimental values are in reasonable agreement; differences in asymmetry change the σ_{11} value of the tensor. The three sets of principal values are experimental SA (−532, 52, 480), paramagnetic SA (−525, −15, 541), and overall SA (−503, 40, 543).

nances were not observed, presumably because the induced shifts were too small to resolve them from the main peaks in the spectrum.

Three resonances with isotropic shifts centered around 300 ppm in the spectrum of $Eu_{0.1}Y_{0.9}(O_2CCD_3)_3{\cdot}4D_2O$ enriched with ^{13}C at the *carboxyl groups* (Figure 3) are similar in nature; they relax rapidly for this system ($T_1 \approx 400$ ms) and have similar broad spinning sideband patterns. The resonance with an isotropic shift of approximately 260 ppm has the same shift as the chelating and bridging resonance in the stoichiometric sample. It also has a similar shift anisotropy. The peak at 160 ppm is distinct, having a smaller shift anisotropy than those at 300 ppm and a longer T_1 of approximately 2 s. Assignments made on the basis of T_1's and by analysis of data extracted from the envelope of the spinning sidebands (*vide infra*) are summarized in Table III for all the compounds and solid solutions studied.

In the spectrum from $Eu_{0.1}Y_{0.9}(O_2CCD_3)_3{\cdot}4D_2O$ selectively enriched in ^{13}C at the *methyl* groups (Figure 4), broadened resonances at the chemical shifts found in $Y(O_2CCH_3)_3{\cdot}4H_2O$ are again observed, and additionally there are two paramagnetically shifted resonances, at −35 and −45 ppm, in the ratio 1:2. While the resonances fall at the same shifts as observed for $Eu(O_2CCD_3)_3{\cdot}4D_2O$, their shift anisotropies differ markedly, and X-ray microanalysis did not show the presence of separate phases. Hence the resonances observed do not result from traces of stoichiometric $Eu(O_2CCD_3)_3{\cdot}4D_2O$ but from the solid solution.

3.3. ^1H MAS–NMR Spectra. ^1H MAS spectra have been obtained from samples of the tetraacetates of yttrium, samarium, and europium. To reduce homonuclear dipolar coupling to a level where it could be removed by MAS, the residual protons in samples which were largely deuterated were studied.[14] In practice, problems of sensitivity and background signals meant

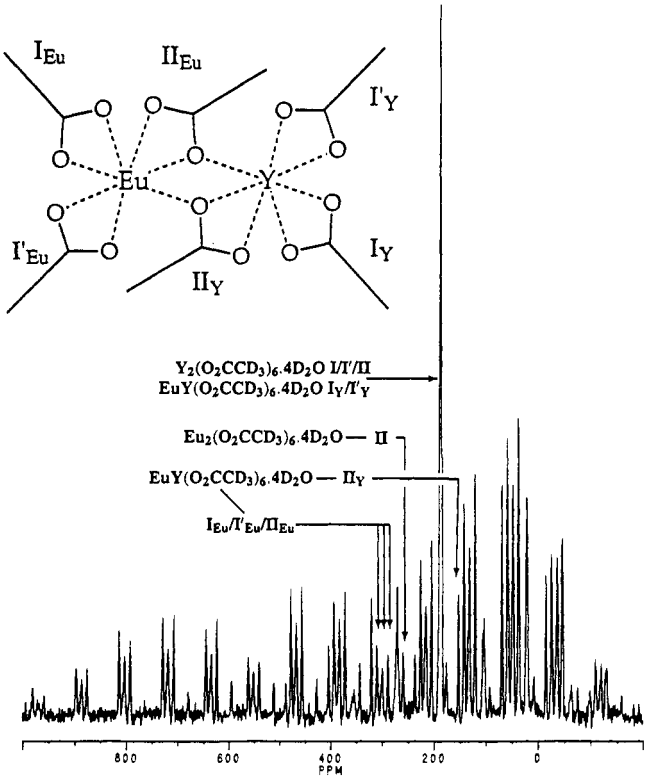

Figure 3. ^{13}C MAS–NMR spectrum of $Eu_{0.1}Y_{0.9}(CD_3CO_2)_3{\cdot}4D_2O$, labeled in ^{13}C at the carbonyl group and collected at a spinning speed of 4800 Hz. The spectrum was processed with 50 Hz of resolution enhancement; labels indicate the isotropic resonances and follow the notation indicated in the schematic diagram of a $EuY(O_2CCD_3)_3{\cdot}4D_2O$ dimer also shown in this figure. SA tensors obtained by analysis of this spectrum and estimates of distances are given in Table III.

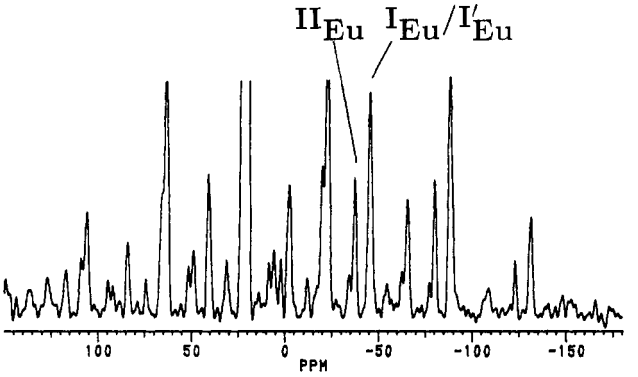

Figure 4. ^{13}C MAS–NMR spectrum of $Eu_{0.1}Y_{0.9}(O_2CCD_3)_3{\cdot}4D_2O$, ^{13}C labeled at the methyl group, acquired at 9.4 T, and collected at a spinning speed of 4275 Hz. SA tensors obtained by analysis of this spectrum and estimates the distances are given in Table III. The spectrum was processed with 50 Hz of resolution enhancement.

that 3% of protonated acetate groups needed to be introduced to obtain reasonable spectra. A ^1H spectrum is shown in Figure 5 for the case of $Sm(O_2CCD_3)_{2.91}(O_2CCH_3)_{0.09}{\cdot}4D_2O$. Attempts to acquire a ^1H spectrum from $Eu(O_2CCD_3)_{2.91}(O_2CCH_3)_{0.09}{\cdot}4D_2O$ were not successful; the line widths observed were greater than obtainable spinning speeds which, combined with the large spread of spinning sideband envelopes in excess of 100 kHz, resulted in severely distorted spectra that could not be reliably phased.

3.4. Simulation of Spinning Sideband Envelopes. The large spinning sideband manifolds observed in the ^{13}C spectra of the paramagnetic lanthanide acetates result primarily from contributions from the CSA and the anisotropic part of the hyperfine shift. The contribution to the hyperfine shift from the dipolar

Table III. Isotropic Shifts, Experimental Overall Shift Anisotropy Tensors, and Estimates of Distances for the Compounds $Ln(O_2CCD_3)_3{\cdot}4D_2O$ (Ln = Eu, Pr, Nd) Selectively Enriched in ^{13}C at the Methyl (Me) or Carboxyl (CO) Groups[a]

Ln	enriched carbon	site	σ_{iso}	Δ	η	predicted distance, Å	$Y(O_2CCH_3)_3{\cdot}4H_2O$ distance, Å
Eu	CO	$I_{Eu}/I'_{Eu}/II_{Eu}$	290, 300, 310	690	0.35	2.30	2.32/2.25
	CO	II (Eu_2 dimer)	260	*b*	*b*	*b*	*b*
	CO	II_Y	150	360	0.40	2.85	2.83
Eu	Me	II_{Eu}	−35	140	0.7	4.93	4.41
	Me	I_{Eu}/I'_{Eu}	−45	145	0.54	4.86	4.35
Pr	CO	II_Y	218	360	0.35	2.85	2.83
	CO	I_{Pr}/I'_{Pr}	158	760	0.15	2.26	2.25
	CO	II_{Pr}	130	660	0.25	2.36	2.32
	CO	I_{Pr}/I'_{Pr}	128	740	0.25	2.26	2.25
Pr	Me	$I_{Pr}/I'_{Pr}/II_{Pr}$	42, 47, 52	148	0.45	4.83	4.35/4.41
Nd	Me	II_{Nd}	50	150	0.1	4.81	4.41
	Me	I_{Nd}/I'_{Nd}	57	150	0.2	4.66	4.35

[a] Assignments of the resonances have been made on the basis of these distances; distances in the host structure, $Y(O_2CCH_3)_3{\cdot}4H_2O$, are given for comparison. Values of Δ and η for the methyl groups resonances were calculated from spectra acquired at both 4.7 and 9.4 T. [b] The signal-to-noise ratio for these resonance was too low to permit analysis; the spinning sideband envelope is, however, similar to that observed for the resonance at the same shift in $Eu(O_2CCD_3)_3{\cdot}4D_2O$.

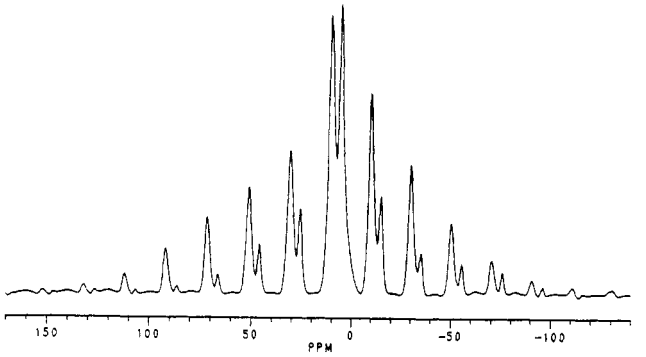

Figure 5. ^1H MAS–NMR spectrum of $Sm(O_2CCD_3)_3{\cdot}4D_2O$ containing approximately 3% protonated acetate groups and collected at a spinning speed of 4000 Hz.

coupling of electronic and nuclear spins $\Delta\mathcal{H}^d$ was calculated as follows[27]

$$\Delta\mathcal{H}^d = \bar{\mu}_e D_{en} \mu_n = \gamma_n \bar{\mu}_e D_{en} I_n$$

where $\bar{\mu}_e$ is the time averaged magnetic moment of the paramagnetic ion and D_{en} is the dipolar coupling tensor. For a single nucleus interacting with one paramagnetic center,[45] the shift tensor $(\Delta\mathcal{H}/\mathcal{H}_o)^d$ is given by

$$(\Delta\mathcal{H}/\mathcal{H}_o)^d = \frac{-(1 - 3\hat{r}\cdot\hat{r})}{4\pi r^3}\chi$$

where $\hat{r}$ is the vector joining the observed nucleus to a given paramagnetic center, and χ is the atomic magnetic susceptibility tensor. Assuming that the magnetic properties of the lanthanide ions in the acetates are identical to those for the free ions, then χ is isotropic (and can be calculated[45]). The total dipolar coupling tensor, for a particular ^{13}C site, was obtained by summing all the dipolar coupling tensors from each individual Ln–C coupling. Lanthanide ions within a distance of 100 Å from the atom of interest were included in this sum. Summation up to this distance was needed for convergence. Values for $(\Delta\mathcal{H}/\mathcal{H}_o)^d$ for the protons in these structures were also calculated in a similar fashion. Methyl group rotation and 180° flips of the water molecules were allowed for by averaging over the sites in fast exchange within the methyl groups and the water molecules, respectively. The calculated values of $(\Delta\mathcal{H}/\mathcal{H}_o)^d$ for the ^{13}C and ^1H atoms in the stoichiometric compounds obtained in this way are given in Table II.

The experimental spectra were then simulated, assuming $(\Delta\mathcal{H}/\mathcal{H}_o)^d$, which we refer to as the paramagnetic shift anisotropy, to be the dominant source of the anisotropy, and Figure 2d shows the results for $Eu(O_2CCD_3)_3{\cdot}4D_2O$. Simulations were also performed in which the CSA tensor was added to the hyperfine tensor to provide a better approximation to the observed spectra. The ^{13}C CSA tensors were measured by analysis of slow spinning CPMAS–NMR spectra of $Y(O_2CCH_3)_3{\cdot}4H_2O$ and were aligned relative to the acetate groups using the orientations determined in the single crystal NMR study of $Cd(O_2CCH_3)_2$.[46] The overall shift anisotropy tensors calculated in this way are given in Table II.

It is more complicated to calculate values for $(\Delta\mathcal{H}/\mathcal{H}_o)^d$ for the solid solutions. A range of local environments will contribute that contain differing distributions of paramagnetic ions in more distant coordination spheres. The hyperfine tensors would have to be determined individually for each local environment and then summed. We attempted this operation by assuming that the paramagnetic ions were distributed randomly in the lattice and summed spectra from a large number of different determinations of the SA. The amount of computer time required, however, proved prohibitive, and we have instead chosen to simplify the problem by assuming the solid solutions to be sufficiently dilute that each ^{13}C site interacts with only one paramagnetic center. Considering the ^{13}C sites within a $M_2(O_2CCD_3)_3{\cdot}4D_2O$ dimeric unit containing a paramagnetic ion, the shift anisotropy will be dominated by coupling to this one paramagnetic moment; $(\Delta\mathcal{H}/\mathcal{H}_o)^d$ will be axial with principal components given by

$$10^6(\Delta\mathcal{H}/\mathcal{H}_o)^d_{\parallel}/\text{ppm} = 2\chi/4\pi r^3;$$

$$10^6(\Delta\mathcal{H}/\mathcal{H}_o)^d_{\perp} = -\chi/4\pi r^3$$

The results shown in Table III were obtained using this approximation.

4. Discussion

In the previous sections we have shown that by the use of deuterated samples it is possible to obtain well resolved ^{13}C and ^1H MAS–NMR spectra from the stoichiometric lanthanide acetate tetrahydrates of samarium, neodymium, and europium. Additionally we have been able to obtain well resolved spectra from solid solutions containing only small amounts of lanthanide ions substituted for yttrium ions in a host of deuterated yttrium acetate tetrahydrate. It is possible to measure isotropic and anisotropic shifts and also to measure the line widths of the individual spinning sidebands in these spectra. We now investigate the factors determining the form of these spectra and consider the possibilities for the use of paramagnetic ions in analysis of solid-state structures.

4.1. Isotropic Shift Mechanism. Shifts in the resonant frequencies of nuclei surrounding paramagnetic species can result from two sources. They may be induced by interactions through the bonding electrons, resulting in contact shifts, or by through space dipolar coupling to an anisotropic magnetic moment, resulting in pseudocontact shifts.[47]

For the lanthanide compounds considered in this paper, the only significant through bond interaction is the Fermi contact

(44) Raleigh, D. P.; Grey, C. P.; Soffe, N.; Dobson, C. M. *J. Magn. Reson.* **1992**, *97*, 162.
(45) Bleaney, B. *J. Magn. Reson.* **1972**, *8*, 91.
(46) Ganapathy, S.; Chacko, V. P.; Bryant, R. G. *J. Chem. Phys.* **1984**, *81*, 661.
(47) Figgis, B. N. *Introduction to Ligand Fields*; Wiley-Interscience: 1966.

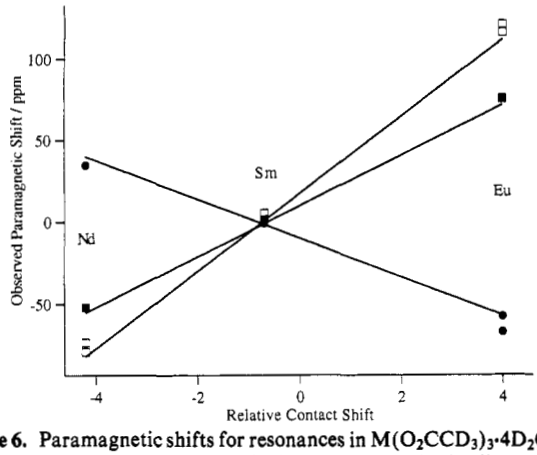

Figure 6. Paramagnetic shifts for resonances in $M(O_2CCD_3)_3{\cdot}4D_2O$ (M = Sm, Nd, Eu) relative to the equivalent resonances in the diamagnetic compound $Y(O_2CCH_3)_3{\cdot}4H_2O$, plotted against the expected relative contact shift. Open squares represent type I/I′ carbonyl groups; filled squares represent type II carbonyl groups; circles represent methyl groups. For a Fermi contact mechanism, the shift is expected to be given by $\Delta\mathcal{H}_j = (A_n \langle S_Z \rangle)/(g_n\beta_n)$,[48] where g_n is the nuclear gyromagnetic ratio, a_n is the nuclear hyperfine coupling constant, and $\langle S_z \rangle$ is the averaged z component of the rare earth electronic spin. The nonzero intercept of the graph may imply some contribution to the shifts from a pseudocontact mechanism.

shift.[48] This is proportional to $\langle S_Z \rangle$, the averaged z component of the spin on the paramagnet, and to the hyperfine coupling constant which depends on the extent of orbital overlap. The pseudocontact shift results from dipolar coupling to an anisotropic magnetic moment. It has been shown to depend on $g_z \langle J \| \alpha \| J \rangle J(J+1)(2J-1)(2J+3)$[45] and a term depending upon the geometry of the system.

It is not possible to differentiate between these two shift mechanisms on the basis of the temperature dependence of the shifts for a single compound, since the factors determining this temperature dependence are complex, particularly for the lanthanide ions studied here. For Eu^{3+}, low-lying excited electronic states are thermally occupied, and for Sm^{3+} there is mixing in of excited electronic states into the ground state. We have not acquired variable temperature spectra for the Nd^{3+} compound, since we have been unable to prepare a sufficiently pure sample.

It is necessary instead to consider correlations between the shifts for a series of homologous compounds. The contact shifts for the compounds $Ln(O_2CCD_3)_3{\cdot}4D_2O$ (Ln = Y, Sm, Eu, Nd) are found to correlate approximately with $\langle S_Z \rangle$, as shown in the graph in Figure 6, but not with $g_z \langle J \| \alpha \| J \rangle J(J+1)(2J-1)(2J+3)$. This suggests that the dominant contribution to the paramagnetic shifts is from the contact mechanism and that the hyperfine constant is approximately the same for all the compounds in the series. The latter is reasonable since the geometry of the lanthanide ions is similar for all the tetrahydrates. In particular it is important to note that the paramagnetic shifts for the ions Nd^{3+} and Eu^{3+} are in opposite directions; this is consistent with a contact interaction, whereas a pseudocontact interaction would be expected to result in paramagnetic shifts in the same direction for these two ions.

It is possible, however, that the contact interaction is not the only contribution to the observed shifts. The magnitude of the small difference in shift between the type I and I′ carbonyl resonances for the lanthanide acetate tetrahydrates of neodymium, samarium, and europium is found to correlate with the magnitude of $g_z \langle J \| \alpha \| J \rangle J(J+1)(2J-1)(2J+3)$; this indicates that there may be a small pseudocontact contribution to the shift resulting from dipolar interactions.

(48) Golding, R. M.; Halton, M. P. *Aust. J. Chem.* **1972**, *25*, 2577.

We assume that the shifts are determined predominantly by a through bond contact mechanism. Hence, in considering shifts for a particular acetate group we only consider interactions with metal ions coordinated to that acetate group; we neglect long range through space interactions. In a $M_2(O_2CCD_3)_6{\cdot}4D_2O$ dimer, carbon atoms in type I and I′ acetate groups will experience shifts from only one metal ion, while carbon atoms in type II (bridging) groups can experience a contact shift from either or both metal ions. It is possible to distinguish between these different interactions by investigating the shifts observed in the spectra of the solid solutions, $Ln_xY_{(1-x)}(O_2CCD_3)_3{\cdot}4D_2O$ ($x \leq 0.1$). If there is no ordering of the different cations in these solid solutions, then the majority of $M_2(O_2CCD_3)_6{\cdot}4D_2O$ dimers will contain two yttrium ions, some will contain one yttrium ion and one lanthanide ion, and a very small fraction (≤1%) will contain two lanthanide ions. Hence, the major set of paramagnetically shifted resonances will arise from the dimers containing one lanthanide ion and one yttrium ion. All six acetate groups will be inequivalent in these $LnY(O_2CCD_3)_6{\cdot}4D_2O$ dimers, and it should be possible to observe contact shifts to the type II (bridging) groups from either the metal atom to which they are bidentate (chelating) or monodentate (bridging).

Table III shows assignments for the resonances observed in the MAS–NMR spectra of the solid solutions $Ln_xY_{(1-x)}(O_2CCD_3)_3{\cdot}4D_2O$ ($x \leq 0.1$) made both on the basis of the isotropic shifts discussed in this section, and on the basis of the line widths and shift anisotropies discussed later. These assignments enable calculation of the approximate contact shifts for the various sites, by subtraction of the chemical shifts for the resonances of the equivalent groups in the homologous diamagnetic compound, $Y(O_2CCH_3)_3{\cdot}4H_2O$. Two type I_{Eu}/I'_{Eu} and one type II_{Eu} (bridging to an yttrium ion in the dimer) acetate groups directly bonded (bidentate) to an europium experience a contact shift to the carboxyl group of 104, 114, or 124 ppm (average 114 ppm), while the other type II_Y (bridging) carboxyl group that is directly bonded (bidentate) to an yttrium ion but bridging (monodentate) to an europium ion experiences a smaller contact shift of −36 ppm.

The contact shifts obtained from spectra of $EuY(O_2CCD_3)_6{\cdot}4D_2O$ dimers in $Eu_{0.1}Y_{0.9}(O_2CCD_3)_3{\cdot}4D_2O$ can be used to obtain estimates of the contact shifts for carbonyl groups in the *stoichiometric* compound $Eu(O_2CCD_3)_3{\cdot}4D_2O$. The type I and I′ carboxyl resonances will experience contact shifts of approximately 114 ppm from the neighboring Eu^{3+} ion. The type I and I′ carbonyls in the diamagnetic compound resonate at a chemical shift of approximately 189 ppm, and hence the paramagnetically shifted type I and I′ carbonyl atoms are expected to resonate at approximately 303 (= 189 + 114) ppm. The experimental spectrum of $Eu(O_2CCD_3)_3{\cdot}4D_2O$ contains carboxyl resonances in the region 300–310 ppm. The type II (bridging) carboxyl carbon should experience a contact shift of approximately 114 ppm from the Eu^{3+} ion that it chelates and additionally a contact shift of approximately −36 ppm from the Eu^{3+} ion to which it is bridging; this results in an overall predicted contact shift of 78 ppm. Type II (bridging) carboxyl groups have a chemical shift of approximately 186 ppm in the diamagnetic compound and allowing for the contact shift are expected to resonate at 264 (= 186 + 78) ppm; the experimental spectrum has a carboxyl resonance at 260 ppm. These two chemical shift calculations confirm the assignments for the carboxyl resonances in the stoichiometric compound $Eu(O_2CCD_3)_3{\cdot}4D_2O$.

In the spectra of $Eu_{0.1}Y_{0.9}(O_2CCD_3)_3{\cdot}4D_2O$ enriched to 10% in ^{13}C at the carboxyl groups, there is also a resonance of low intensity with an isotropic shift of 260 ppm; we postulate that this results from type II (bridging) carboxyl groups in $Eu_2(O_2CCD_3)_6{\cdot}4D_2O$ dimeric units present in low concentration in $Eu_{0.1}Y_{0.9}(O_2CCD_3)_3{\cdot}4D_2O$. The spinning sideband envelope is similar to that observed for the resonance with a shift of 260 ppm

in the stoichiometric compound, but this resonance in the spectrum from the solid solution has too poor a signal-to-noise ratio for meaningful analysis.

The methyl groups are less readily analyzed, since we observe two peaks with intensities in the approximate ratio of 2:1 at the same shifts (−35 and −45 ppm) in spectra of both the stoichiometric compound and the solid solution. We postulate that this is because the Fermi contact interaction with a monodentate type I^r (bridging) group is too small to be observed, and hence the thre methyl groups around an Eu^{3+} ion appear to experience the same shifts whatever the other ion in the dimer. Similarly, the resonance due to type II (bridging) methyl groups chelated to an yttrium ion but bridging to an europium ion is not resolved presumably because the contact shift it experiences is too small to resolve it from the overlapping set of resonances resulting from $Y_2(O_2CCD_3)_6{\cdot}4D_2O$ dimers. Note that while the resonances at −35 and −45 ppm have *isotropic* shifts that are the same as those observed for the stoichiometric compound $Eu(O_2CCD_3)_3{\cdot}4D_2O$, the *anisotropic* shifts differ; these peaks do not reflect the presence of a small amount of the stoichiometric compound. Such a phase was not detected by X-ray emission analysis which showed the solid solutions to be homogeneous.

The results obtained from analysis of the ^{13}C MAS spectra of the solid solutions containing Eu^{3+} ions have therefore enabled calculation of the isotropic shifts observed in spectra of the equivalent stoichiometric compound. Similar calculations are also possible for the case of neodymium ions. Praseodymium acetate does not form the tetrahydrate, so it is not possible to determine if calculation of the spectra of the stoichiometric compound is successful.

4.2. Factors Influencing Line Widths. The results presented in this paper show that the *line widths of individual spinning sidebands* in the ^{13}C MAS–NMR spectra of the protonated paramagnetic lanthanide acetates are larger than those of the homologous diamagnetic compounds (see Table I). It is important, however, to distinguish this effect from the shift anisotropy manifested in the *spinning sideband envelope* for a particular resonance, or in spectra of static (i.e., nonspinning) powders, which is generally a much larger interaction. A possible cause of the linebroadening in paramagnetic compounds is fast nuclear relaxation, induced by coupling to electronic moments on adjacent paramagnetic centers. It has been shown, however, that for the stoichiometric lanthanide acetates (Ln = Ce–Eu), nuclear relaxation only accounts for a small proportion of the large observed line widths.[12] Electron relaxation in these compounds would appear to be too fast to induce significant nuclear relaxation. ^{13}C T_1 and T_2 values in these compounds are reduced relative to the analogous diamagnetic materials, but broadening from this source accounts for only a small fraction of the observed line widths. For Gd^{3+}, electronic relaxation is much slower because of the f^7 electronic configuration; it has not been possible to obtain resolved spectra from compounds containing this ion.

The CP-MAS spectra of the proton-containing acetates were collected under conditions of ^1H decoupling. For such decoupling to be effective, however, the ^1H nuclei must couple strongly with the external radiofrequency field. For paramagnetic compounds the large anisotropy of the ^1H shift may result in the decoupling field being significantly off resonance for most of the rotor period. The simulated SA for the methyl protons in $Sm(O_2CCH_3)_3{\cdot}4H_2O$ spans 40 kHz, in agreement with the experimental proton spectra of $Sm(O_2CCD_3)_{2.91}(O_2CCH_3)_{0.009}{\cdot}4D_2O$. For $Eu(O_2CCH_3)_3{\cdot}4H_2O$, the calculated SA spans 200 kHz, though it was not possible to confirm this experimentally. Calculations following Vanderhart, Earl, and Garroway[49] suggest that with the decoupling fields of about 60 kHz achievable with our MAS probes an SA of this magnitude would lead to incomplete proton decoupling, with contributions to the line widths of approximately 700 and 1100 Hz for the methyl carbons in $Eu(O_2CCH_3)_3{\cdot}4H_2O$ (cf. the observed line widths of about 1200 Hz). This is confirmed by the success of techniques such as RSVP in reducing line widths.[42,43,44,50]

Even in the absence of dipolar interactions, for any paramagnetic sample in a uniform external field, there will be a distribution of internal fields, because of the effects of the difference in susceptibility between the powder and the surrounding air and because of the nonuniform shapes of the particles.[49,51-53] To first order, this broadening of the isotropic resonance under MAS is averaged, although the envelope of the spinning sidebands is distorted. Second-order effects due to anisotropy in the bulk susceptibility remain, however, and have been shown to make a major contribution to the line widths of spectra of a number of compounds. The anisotropic part of the bulk magnetic susceptibility will be reduced by lowering the overall susceptibility, and hence anisotropic bulk magnetic susceptibility (ABMS) broadening will be much lower for the solid solutions of paramagnetic ions in a diamagnetic host than for the equivalent stoichiometric paramagnetic compounds. The results given in Table I show that the line widths in the solid solutions studied here are much smaller than the line widths for the stoichiometric compounds containing the same lanthanide ions; ABMS broadening is likely to be a major reason for this.

Finally linebroadening in solid solutions could arise from chemical inhomogeneities in the samples, due to uneven distributions of species in the second and third coordination shells, or as a result of defects or other inhomogeneities in stoichiometric samples. In the compounds studied in this paper, however, broadening from inhomogeneities must be small, since the observed line widths of the deuterated solid solutions are small and can be accounted for largely by ABMS broadening.

The results obtained indicate therefore that the major contribution to the isotropic peak line widths in ^{13}C MAS–NMR spectra of paramagnetic lanthanide acetates not containing protons is from ABMS broadening; for proton containing compounds, there is an additional large contribution to the isotropic peak line widths resulting from incomplete proton decoupling.

4.3. Structural Analysis using Shift Anisotropies. In Table II, calculated paramagnetic SA tensors and calculated overall SA tensors for $Eu(O_2CCD_3)_3{\cdot}4D_2O$ and $Sm(O_2CCD_3)_3{\cdot}4D_2O$ are compared with those determined by analysis of experimental spectra. Figure 2 shows the experimental (c) and calculated (d) spectra of $Eu(O_2CCD_3)_3{\cdot}4D_2O$.

For the compound $Eu(O_2CCD_3)_3{\cdot}4D_2O$, the fit between the experimental and calculated results is good. The calculated overall shift anisotropy for the carboxyl groups, allowing both for paramagnetically induced SA and for CSA, is not quite large enough, but the experimental spectra are expected to be slightly broadened by magnetic susceptibility effects. The overall calculated tensor is dominated by the paramagnetic interaction, so that any errors in the magnitude or alignment of the CSA will have a minimal effect; indeed the tensor allowing only for the paramagnetic contribution to the SA and neglecting the contribution from the CSA is still a reasonable approximation to the experimental data. For the methyl groups in $Eu(O_2CCD_3)_3{\cdot}4D_2O$, the fit is less good. The overall SA tensors obtained by analysis of the experimental NMR spectra in this case are only approximate, since the fit had to be performed on small numbers of sidebands, in a crowded spectrum. The paramagnetic contribution to the observed tensor is smaller, and hence errors in the CSA

(49) Vanderhart, D. L.; Earl, W. L.; Garroway, A. N. *J. Magn. Reson.* **1981**, *44*, 361.

(50) Brough, A. R.; Grey, C. P.; Raleigh, D. P.; Dobson, C. M. Unpublished results.

(51) Alla, M.; Lippmaa, E. *Chem. Phys. Lett.* **1982**, *87*, 30.

(52) Drain, L. E. *Proc. Phys. Soc.* **1962**, *80*, 1380.

(53) Ganapathy, S.; Bryant, R. G. *J. Magn. Reson.* **1986**, *70*, 149.

will have a larger effect on the overall tensor. Susceptibility broadening effects will also be more significant.

For $Sm(O_2CCD_3)_3 \cdot 4D_2O$ the fit is quite good for the methyl groups but poor for the carboxyl groups. The reasons for this are not clear; it is possible that the good fit for the methyl groups is fortuitous. The fits between experimental and calculated data are likely to be severely limited for the methyl groups, because the CSA and the overall SA are similar in magnitude; any errors in the magnitude or alignment of the CSA will therefore severely effect the overall calculated tensor. These results confirm that for accurate calculation of the overall tensor when the CSA is not known accurately, the paramagnetic contribution to the overall SA must be dominant. We have shown previously that, in a more simple system,[31] fits can be excellent when this is the case.

In the case of stoichiometric compounds, the paramagnetic contribution to the overall SA is not only determined by the distance between an atom and its nearest neighbor paramagnet but also depends on the positions of more distant lanthanide ions in adjacent unit cells. The use of NMR data to determine the structure of stoichiometric lanthanide compounds in the absence of diffraction data is therefore limited by the effects of dipolar coupling to paramagnetic species in adjacent unit cells. With this in mind, solid solutions have also been investigated with the aim of reducing the effects due to paramagnetic species not in the immediate vicinity of the atom being observed.

The NMR spectrum of the compound $Eu_{0.1}Y_{0.9}(O_2CCD_3)_3 \cdot 4D_2O$ enriched to 10% in ^{13}C at the carboxyl groups and shown in Figure 3 is now considered in detail. The shifts originate from the contact interaction, and hence it is assumed that the paramagnetically shifted resonances result from sites directly adjacent to paramagnetic ions within a predominantly diamagnetic lattice; solid solutions of even greater dilution would make this assumption better but were not used because of the need to obtain spectra with good signal-to-noise ratios. Assuming that the bulk of the material is diamagnetic, it was possible to approximate the dipolar coupling to all the paramagnetic species in the lattice by the dipolar coupling to the nearest neighbor paramagnet, since this is the dominant interaction. This results in an axial tensor (i.e., $\eta = 0$) with

$$\left(\frac{\Delta\mathcal{H}}{\mathcal{H}_0}\right)^{d}_{\parallel} = \frac{2\chi}{4\pi r^3}$$

Clearly this is not an accurate description of the overall shift anisotropy, since the observed tensors are not axial, and the CSA has been neglected; it is, however, useful as a simple first approximation. Since an estimate of the susceptibility can be calculated by assuming the free ion approximation, it is possible to estimate the distance between a ^{13}C nucleus and its nearest neighbor paramagnet from the observed shift anisotropy, neglecting the nonaxial component. Then

$$r \approx \sqrt[3]{\frac{\chi_{iso}}{2\pi} \Big/ \left(\frac{\Delta\mathcal{H}}{\mathcal{H}_0}\right)^{d}_{\parallel}}$$

Using this approach for $Eu_{0.1}Y_{0.9}(O_2CCD_3)_3 \cdot 4D_2O$, carbonyl groups are predicted to lie at distances of 2.32 Å (Δ = 690 ppm) and 2.85 Å (Δ = 360 ppm) from the paramagnetic centers. Assuming simple substitution of the Eu^{3+} ions into the $Y(O_2CCH_3)_3 \cdot 4H_2O$ crystal structure, then in an $EuY(O_2CCD_3)_6 \cdot 4D_2O$ dimer, the directly bonded carbonyl groups I_{Eu}, I'_{Eu}, and II_{Eu} are at distances of 2.25-2.32 Å from the paramagnet, while the carboxyl group II_Y, directly bonded to Y^{3+} but bridging to the Eu^{3+} ion, is at a distance of 2.83 Å from the paramagnet. Thus, agreement is excellent in this case and enables the assignments shown in Table III to be made.

The ^{13}C MAS-NMR spectrum obtained from $Eu_{0.1}Y_{0.9}(O_2CCD_3)_3 \cdot 4D_2O$ enriched to 10% in ^{13}C at the methyl groups (Figure 4) contains two resonances with paramagnetic shifts, at −35 and −45 ppm. These are in the approximate ratio of 1:2 and would appear to result from the three acetate groups directly chelated to Eu^{3+} in an $EuY(O_2CCD_3)_6 \cdot 4D_2O$ dimer. The magnitude of the overall SA (Δ = 140 ppm) suggests that they are at a distance of 4.9 Å, which differs from the actual value of 4.4 Å by 10%. We have been unable to observe a resonance due to the type II_Y methyl groups (in type II ligands that are chelating to an yttrium ion but bridging to an europium ion); this may be attributed to the small contact shift experienced by such groups. It is possible that this resonance is the shoulder to low field of the diamagnetic resonance; we have not been able to analyze the experimental shift anisotropy.

The estimates of distance are surprisingly accurate, despite the gross approximations involved both in ignoring the asymmetric part of the observed overall SA and in neglecting contributions to the overall SA from the CSA and from interactions with paramagnetic species that are not nearest neighbors. This good agreement indicates that the contribution to the overall SA from the nearest neighbor paramagnet is dominant and that the CSA is relatively unimportant. This is reasonable for the carboxyl groups, but for the methyl groups the paramagnetic contribution to the overall SA is smaller and other interactions become more important; the departures from this approximation therefore become larger. The deviations of the tensors from axiality also appear to be larger for the methyl groups than for the carbonyl groups, though it should be noted that the smaller number of sidebands observed in the spectra of the methyl groups means that the overall SA tensors extracted from the experimental data are less reliable. Since the paramagnetic part of the SA scales are the inverse cube of distance, however, distance measurements are relatively unaffected by small changes in the SA. A 15% increase in the SA only changes the estimated distance by 5%. Hence the method may be expected to be reasonably robust, and it should be possible to find applications in a wide range of systems where the bonding is molecular so that long range contact interactions do not occur.

5. Conclusions

The results presented in this paper demonstrate that, under suitable conditions, well resolved spectra can be obtained from crystalline compounds containing paramagnetic ions. Some of the factors increasing line widths of paramagnetic compounds compared to their diamagnetic analogues are considered, and it has been shown that ABMS broadening is the major factor producing broadening in paramagnetic solids that do not contain protons. For proton containing solids there is a large additional contribution to the line widths as a result of incomplete proton decoupling as a consequence of the large proton SA's. We have, however, been able to achieve efficient decoupling by perdeuterating the materials studied, as an alternative to the more sophisticated decoupling schemes required to achieve efficient decoupling over large bandwidths. We have significantly reduced the ABMS broadening by working with dilute solid solutions of paramagnets in a diamagnetic host material. By these means we have been able to obtain spectra with sufficient resolution to analyze the isotropic and anisotropic shifts.

For the stoichiometric compounds, analysis of the isotropic shifts observed for the homologous series of tetrahydrates showed that the contact shift mechanism was predominant. Analysis of the spinning sideband envelopes showed that the overall SA's could be simulated assuming dipolar coupling to the paramagnetic moments; when these were large, the paramagnetic SA was the dominant contribution to the overall SA. For solid solutions we have shown that calculations assuming interactions only involving nearest neighbor paramagnets can give reasonable estimates for the overall observed SA. Since the interaction is then with only

one paramagnet, it is possible to estimate distances directly from the observed tensors. These distances are surprisingly accurate.

In the present work these distances have been used to assign the spectra fully and to determine the feasibility of the approach detailed here. Using these techniques it should be possible both to investigate structures of novel compounds and to obtain information additional to that accessible from NMR spectra of diamagnetic materials alone. The use of paramagnetic species as shift reagents in the solid state should be possible, particularly in the study of materials where long range bonding interactions are minimal, enabling simulations of the overall SA to be carried out in a simple manner. Even in less favorable cases, where there is extended bonding, the method might enable structural models to be tested and distributions of ions to be examined.

Acknowledgment. We wish to acknowledge the SERC for the provision of research studentships for A.R.B. and C.P.G. and for a grant toward the provision of NMR equipment. We thank A. Stoker for performing the X-ray analysis, Dr. J. M. Twyman for valuable advice, and Dr A. J. Edwards for producing the diagram shown in Figure 1.